Hindawi
Journal of Engineering
Volume 2021, Article ID 6668095, 11 pages
https://doi.org/10.1155/2021/6668095

Research Article

Regulation of Temperature on Multitrays in an Indirect Solar Dryer (ISD) with Energy Storage and Three Airflow Modes

G. B. Tchaya,[1] **E. Tchoffo Houdji**,[1] **J. H Tchami**,[2] **C. Kapseu**,[3] **and M. Kamta**[2]

[1]*Department of Renewable Energy, National Advanced School of Engineering, University of Maroua, Maroua, Cameroon*
[2]*Department of Electrical, Energetic and Automatic Engineering, National Advanced School of Agro Industrial Sciences, The University of Ngaoundéré, Yaounde, Cameroon*
[3]*Department of Engineering Process, National Advanced School of Agro Industrial Sciences, The University of Ngaoundéré, Yaounde, Cameroon*

Correspondence should be addressed to G. B. Tchaya; tchayaguy@yahoo.com

Received 9 November 2020; Revised 1 November 2021; Accepted 24 November 2021; Published 16 December 2021

Academic Editor: Paolo Castaldo

This work presents the regulation of temperature in an indirect multitrays solar dryer with oriented flux under the irradiance fluctuation. The temperature regulator using a negative temperature coefficient (NTC) as a sensor and fans is designed, and a similar device is also used to measure humidity through a sensor. Inlet and outlet dryer temperature and temperature on the three trays have been recorded with the regulation system according to different airflow modes. Irradiance and humidity have also been recorded. The model of outlet temperature with energy storage was given by using heat transfer equations. The results have shown that in the linking airflow mode, the average temperature on the three trays is $51.3 \pm 1.5^{a°}$C, $52.18 \pm 1.4^{a°}$C, and $51.9 \pm 1.2^{a°}$C, respectively, with 52°C as setpoint temperature and NTC fixed on tray number 2. With temperature sensor in the same tray and 51°C as setpoint temperature, the average temperatures on the three trays are 51.86 ± 1.54°C, 51.60 ± 1.16°C, and 50.42 ± 1.13°C, respectively, in mixed mode, whereas in crossing airflow mode, the temperature gradient does not allow regulation on all trays. The regulation is possible when the temperature in the dryer chamber exceeds the set point temperature by more than 5%. The proportional type corrector is suitable for the temperature controller in indirect solar dryers. When the energy source is unstable, humidity which is a variable parameter is used to mark the end of drying instead of time.

1. Introduction

Generally, regulation helps to stabilize unstable systems, increase accuracy, productivity, and control production quality, and improve the flexibility of the production chain. Particularly, in agro-food, it improves hygiene (less staff) and limits the effects of final product variability [1–3].

Regulation is well-known and mastered in industrial because the energy source is stable. Generally, the control chain is curly. The difference of temperature between the order temperature and the desired temperature is determined [4]. This is not the case for equipment power by renewable energy sources such as the solar or wind energy system because of their intermittent nature.

The solar drying equipment for agricultural products has been improved with the introduction of new equipment as the integration of heat storage systems such as biomass [5–7], sensible heat energy [8, 9], thermochemical reactions or phase change materials [10–12], and the regulation obtained with hybrid sources [13–15]. However, the sizing and design rules of this process are still insufficient so that these structures meet farmers' expectations [16, 17]. Though different solar dryer designs are now available in Africa for both direct and indirect drying chamber designs [3, 18], research studies to seek new design are still going. Simotagne et al. [19], for example, recently proposed a new indirect solar dryer with collector consisting of conical and parabolic solar concentrator. They found that the parabolic concentrator had comparatively poor drying kinetics when

compared with conical concentrators, while coaxial design outperformed the noncoaxial design for drying kinetics. Modelling and numerical simulations solar dryers are one of the promise means on the way to seek the best solar dryer for different products to dry [8, 20–22].

In general, food products are dried at a fix temperature between 45°C and 60°C [23–26]. This temperature range is obtained without difficulty when the energy source is electric (in the case of equipment in industrial sectors); but, this becomes difficult with solar-thermal source because of their dependence on weather and climate conditions.

If the drying temperature and humidity ranges are known using the control of the drying parameters of food products, the dried products will be in good quality [27–29]. Smart sensors using the fuzzy logic-based control system are increasingly used to master the drying parameters (temperature and humidity in particular) [30, 31], but for populations of rural areas, this type of control system would make the dryer more expensive. So, the classical control theory with low-cost temperature and humidity sensors are used to build the regulation control system for indirect solar dryers to reduce their costs [3]. This approach is used in this work to control the temperature and humidity in an indirect multitrays solar dryer with oriented flux.

2. Materials and Methods

2.1. Measuring Equipment. Data acquisition is done by an acquisition station (ALMEMO 2690–8). It allows storing the drying parameters with the appropriate sensors every five minutes. The measurements of the parameters were made using sensors of temperature (NiCr-Ni thermocouple), humidity (FHAD 46), and irradiance (Lux Probe Head FLA 603), all connected to the ALMEMO.

2.2. Synoptic of Indirect Solar Dryer. Figure 1 shows the model of the dryer used for the experiments. It consists of three compartments (solar collector, drying chamber with three trays, and chimney). However, the chamber gives the possibility of drying in three different ways based on the air circulation mode. Thus, we can distinguish the crossing, licking, and mixed mode.

The first experimentation was carried out to characterize the equipment without regulation. It consists of measuring temperature at inlet and outlet of the solar collector, in the absorber and the irradiance. The curves are presented as function of time.

Figure 2 shows the design of the indirect solar dryer with dimensions of different compartments. The volume of the drying room is 0.125 m^3. The chamber has three trays with 20 cm between two trays.

2.3. Synoptic of the Regulated Dryer with Solar Energy Source. The synoptic diagram (Figure 3) gives the relations between different compartments. We have the sun that provides all the energy available for the whole system, namely, solar-thermal through the glass v, black volcanic stone, and solar photovoltaic, through solar cells.

Then, the fan (3W, 12V, 16.94 g/s) will act as a hot air speed controller in the dryer (enclosure where the product is exposed) through the control (regulator).

Ventilation control varies the temperature and humidity simultaneously because there is only one control parameter. Since the two parameters are linked, it will be a question of regulating the temperature and measuring the path 1 comprising the sun, absorber, glass, and/or storage, and drying chamber is commonly used; path 2 including the solar, cell photovoltaic (30 Wc), control unit, fan, absorber, glass, and/or storage, and drying chamber ensures the control of temperature and measurement of humidity.

Table 1 provides properties of the material used in the solar system.

2.4. Instrumentation. It presents the various measurement sensors and transmitters involved in the conversion of random (nondeterministic) signals. We cannot predict their evolution until we have observed them. Consequently, they can only be described by their statistical properties.

As shown in Figure 4, we will control the humidity to mark the end of the drying by emitting a sound signal, and the renewal of the air will regulate the temperature. Because, it is the same actuator that controls the process.

2.5. Temperature and Humidity Control in the Dryer. The temperature control and the humidity measurement in the forced convection dryer are done, as shown in Figure 5. A humidity sensor and a temperature sensor are placed in a system (process) to send the physical information to a processing circuit in order to realize the regulation loop. Indeed, the excess of moisture in the dryer chamber involves condensation, and the renewal of air in it influences the temperature. This means that because the two parameters are related, regulating the humidity by ventilating strongly influences the stabilization of the temperature. Thus, Figure 4 shows the regulation of the temperature and the measurement of the relative humidity to fix the end of drying of the product. This experiment was performed by Kamta et al. (2010) in an indirect solar dryer with crossing mode and one tray. The temperature is regulated in a range of $T_{\max}$ to $T_{\min}$ corresponding to the supply voltages $V_{c\max}$ and $V_{c\min}$ of the fans. The set temperature T_c corresponds to the voltage V_c given by the following formula:

$$V_c = \frac{V_{c\max} + V_{c\min}}{2}. \quad (1)$$

Experience has shown that this range is optimal for a difference of 2°C around the set point T_c [33].

Here, the negative temperature coefficient (NTC) as sensor closes the loop and thus performs the regulation, while the humidity sensor (HIH 4030 humidity type) is on an open-loop chain and allows a measurement to be made to control the end of the process. This control will sound a buzzer if the humidity set point V_{ch} is reached.

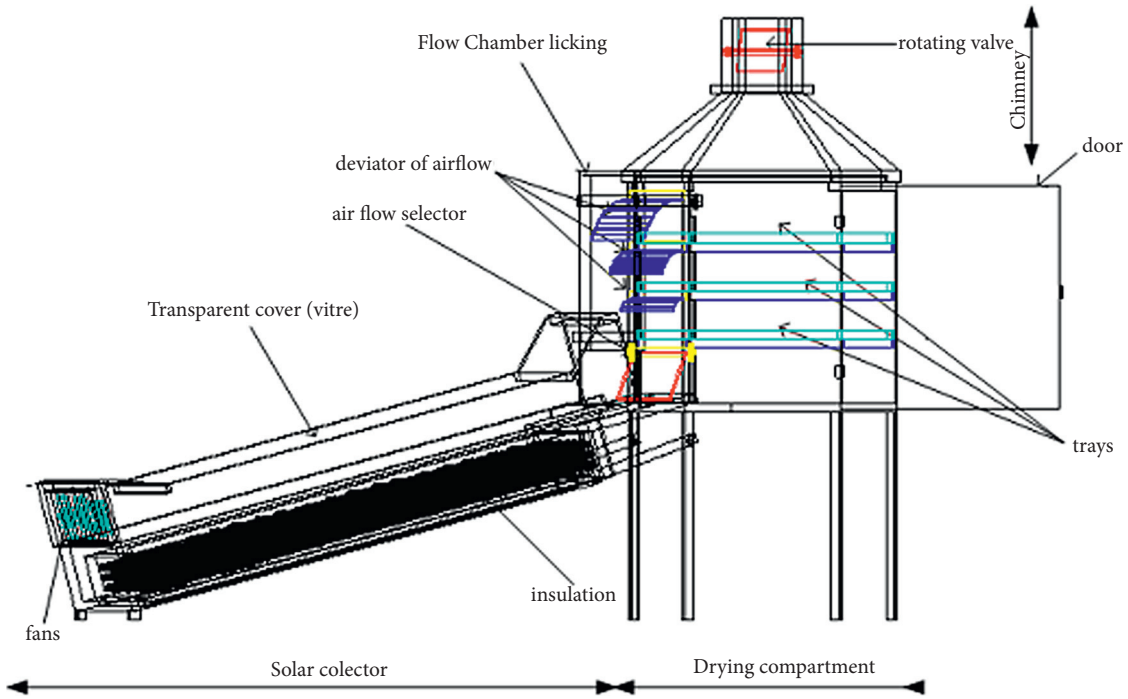

Figure 1: Indirect solar dryer with airflow oriented (ISDAO) [32].

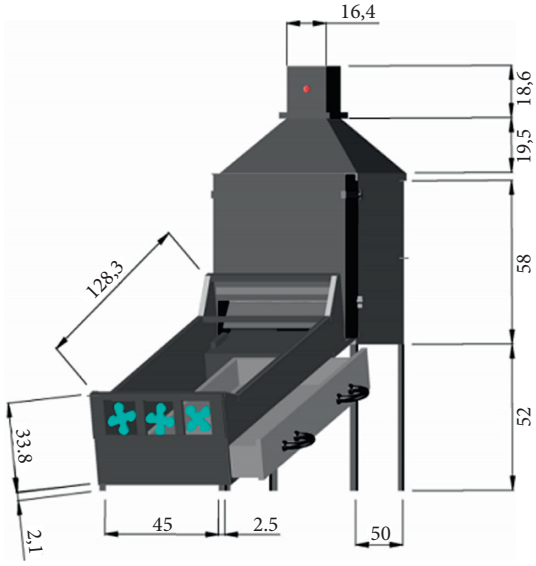

Figure 2: Design of the indirect solar dryer.

Let us consider the thermal sensor as a black box whose input parameters and output parameters are known. Figure 6 shows the thermal phenomena in the solar collector when it receives sunshine, ambient temperature, and ambient relative humidity.

By making a thermal balance on the air, we can express, as a function of time, the equation of the temperature of the outlet air $T_{fs}(t)$ and compare it with the theoretical curve to explain the present phenomenon.

$$m_a c_{pa} \frac{dT_{fs}}{dt} = Sh_n\left(T_n - T_{fs}\right) + Sh_v\left(T_v - T_{fs}\right), \quad (2)$$

where m_a is the mass of air (kg), c_{pa} is the specific heat of the air (J./kg.K), T_{fs} is the inlet fluid temperature (°C), t is the time (s), S is the surface (m^2), h_n is the conductivity heat transfer coefficient (W/m^2 °C), T_n is the absorber plate temperature (°C), h_v is the convective heat transfer coefficient (W/m^2 °C), and T_v is the cover temperature (°C).

2.6. Determination of Heat Exchange Coefficients. Convection exchange coefficient is given in the following equation, where D_h is the characteristic length (hydraulic diameter).

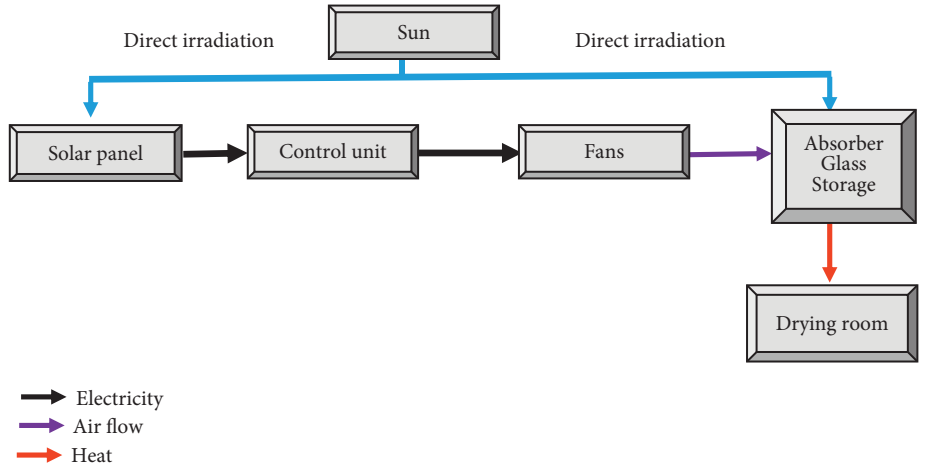

Figure 3: Synoptic of the regulated dryer with solar energy source.

Table 1: Thermophysical properties of materials.

	Calorific capacity ($J \cdot kg^{-1} \cdot K^{-1}$)	Density ($kg \cdot m^{-3}$)	Thermal conductivity ($W \cdot m^{-1} \cdot K^{-1}$)	Coefficient		
				Absorption	Reflection	Emissivity
Steel	465	7833	54	0.95	0.05	0.98
Aluminium	896	2707	204			
Glass	700	2500	1	0,1		0.04
White wood	3147	375	0,12			

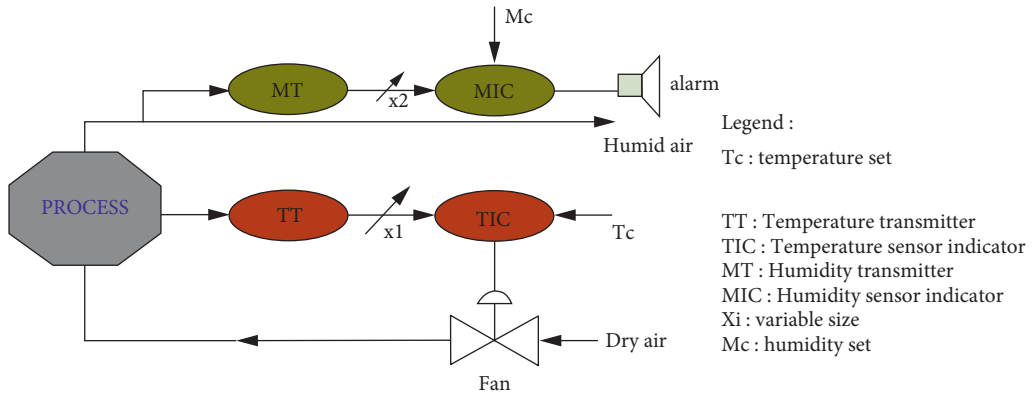

Figure 4: Instrumentation diagram.

$$h_v = \frac{N_u \lambda_f}{D_h}. \tag{3}$$

This convection coefficient is performed by considering the predominant natural convection [34].

In the case where the fluid circulates on a plate inclined at an angle α, the calculation of the Nusselt number is expressed.

For an inclined plate, if $\alpha < 80^\circ$, $10^5 < G_{rL} P_r < 10^{11}$, and the heating surface facing down,

$$N_u = 0.56 \left(G_{rL} P_r \cos \alpha\right)^{1.4}, \tag{4}$$

where G_r is the Grashof number, N_u is the Nusselt number, P_r is the Prandtl number, R_e is the Reynolds number.

Conduction exchange coefficient is

$$h_n = \frac{\lambda_n}{e_n}. \tag{5}$$

2.7. Determination of the Temperature Controller's Model. Figure 7 shows the block diagram of the process in order to propose an ideal regulator to adapt in such a way to ensure a compromise between accuracy and speed. Using the PID

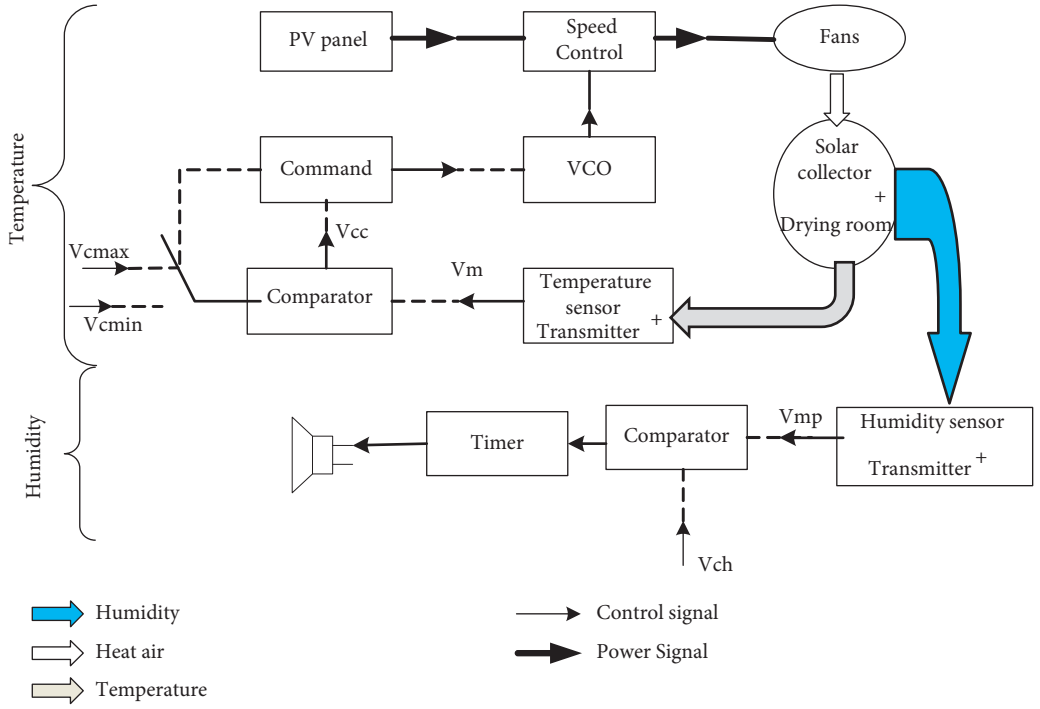

Figure 5: Diagram of electrical control of temperature and relative humidity.

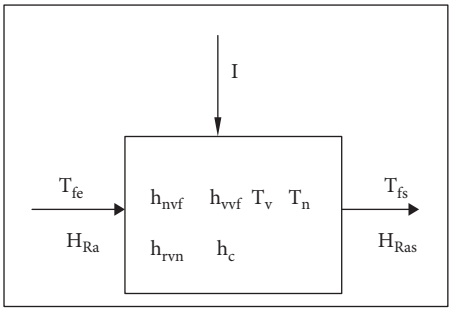

Legend

I : irradiance ;

Tfe : inlet temperature;

HRa : inlet humidity;

Tfs: outlet temperature;

HRas : outlet humidity;

Tn: absorber plate temperature;
Tv: cover temperature;
hc: conductivity heat transfer coefficient;
hrvn: radiative heat transfer coefficient between cover and absorber;
hvvf: Convective heat transfer coefficient between cover and fluid

Figure 6: Phenomenon of solar energy transformation in the thermal collector.

corrector setting by the reference model (Granjon, 2010), the following equations are obtained.

$$F(p) = \frac{X(p)}{W(p)} = \frac{K(p)H(p)}{1 + K(p)H(p)}, \quad (6)$$

$$K(p) = \frac{F(p)}{H(p)[1 - F(p)]}. \quad (7)$$

According to Prouvost [35], one can apply the ideal criteria by expressing the transfer function as

$$F(p) = \frac{1}{1 + \theta_d p}. \quad (8)$$

By replacing equation (5) in (4), the new equation is

$$K(p) = \frac{\theta}{G_s \theta_d} \frac{1 + \theta p}{\theta p}. \quad (9)$$

By identification with the type of corrector, the PID setting to be designed is actually a PI series with following characteristics.

$$K(p) = G_r \frac{1 + T_i p}{T_i p} \; avec \; G_r = \frac{\theta}{G_s \theta_d} \; et \; T_i = \theta. \quad (10)$$

By applying a PI corrector, we can make a good regulation.

By replacing $T_{fs}(p)$ with $X(p)$, we can define the transfer function $H(p)$.

$$H(p) = \frac{X(p)}{Y(p)} \text{ with } Y(p) = \frac{C}{p}; X(p) = \frac{T_{fs}}{p(1/Cp + 1)}, \quad (11)$$

$$H(p) = \frac{G_s}{(1/Cp + 1)}, \quad (12)$$

where

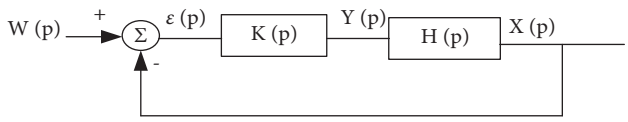

Figure 7: Block diagram of regulation giving the transfer function.

$$G_s = \frac{T_f}{C}, \tag{13}$$

is the static gain of the system

$$\theta = \frac{1}{C} \text{ (time constant)}. \tag{14}$$

In the transfer equation, there is no integration, and the process is said to be naturally stable or self-regulating, according to the Streje model.

3. Results and Discussion

3.1. Regulation of Temperature

3.1.1. Characteristic of the Dryer. It is shown on Figure 8 that for 250 minutes after exposing the dryer on the sun, the average absorber temperature is 75°C when the average irradiance is 700 W/m^2. However, the fluctuation of the irradiance of the outlet absorber temperature is up to 50°C.

3.1.2. Temperature Regulation of the Vacuum Chamber in Crossing Mode. Figure 9 shows that during 2.2 hours, the temperature was kept stable in the three trays at 40.60 ± 1.06°C, 39.42 ± 0.83°C, and 36.15 ± 0.71°C, respectively. Thus, there is a nonuniform temperature distribution in the multitrays indirect solar dryer for the crossing mode with regulation. It should be noted that during the handling period, the irradiance was fluctuated, but since it was sufficient to provide the necessary energy, it could be regulated without difficulty. The average ambient temperature is 31°C. The differences between the temperatures on each stray during the test show the difficulty to uniformly removal moisture on crops inside a multitray solar dryer within a limited time [36]. This would also affect the drying performance when the crop would be introduced in the drying chamber. In fact, without the control system, trays near to the outlet of the solar collector, corresponding to the entry of the drying chamber, have higher drying potentials compared to those situated far from that entry [37, 38].

3.1.3. Influence of the Position of the Sensor (NTC) on the Temperature Control. Table 2 provides the average air temperatures on the trays for different positions of the temperature sensor (NTC) in relation to the trays in order to find the best position for good regulation. For the crossing mode, there is a vertical gradient of temperature, and the position of the NTC does not make it possible to regulate on the trays while keeping this gradient. As for the crossing mode, we will choose the optimal position that gives the best results by licking mode. It is noted that for good temperature regulation, the temperature sensor (NTC) should be placed on the tray 2. The same result is observed in the case of mixed mode.

3.1.4. Temperature Regulation of the Vacuum Chamber in Licking Mode. In licking mode, the temperatures are the same on the three trays with the same gap. In Figure 10, the temperature is regulated at 52°C. Despite the variation of irradiance, the curve of the temperature presents a flat zone for which the regulation is effective.

3.1.5. Temperature Regulation of the Vacuum Chamber in Mixed Mode. Figure 11 shows the temperatures on the three trays for a day where average sunshine reached 928 W/m^2. The averages temperature on the three trays are 51.86 ± 1.54°C, 51.60 ± 1.16°C, and 50.42 ± 1.13°C. The temperature is regulated to the value of 51°C as a set point, and it remained there between 11 h 03 and 14 h 48. The average ambient temperature is 40.5°C.

3.2. Model of the Corrector of Temperature Controller. The theoretical curve is shown in Figure 12. Normally, it grows to a maximum ideally located at solar noon and then decreases until sunset.

The resolution of equation (2) allows us to have the following expression of the temperature as a function of time which explains the profile of the curve of Figure 12.

$$T_{fs}(t) = T_{fe} + \frac{B}{A\left(1 - e^{-\left(A/m_a c_{pa}\right)t}\right)}, \tag{15}$$

with

$$A = S\left(h_n + h_v\right) \text{ and } B = S\left(h_v T_v + h_n T_n\right). \tag{16}$$

The variation of the temperature strongly depends on the convective exchange coefficients.

Thus, the time constant C can be expressed as

$$C = \frac{A}{m_a c_{pa}}. \tag{17}$$

This constant C depends on the properties of the coolant and the convective exchanges, and it influences the rapid attainment of the maximum temperature.

For average temperature values on the glass and the absorber ($T_v = 37$°C and $T_n = 60$°C), the curve (Figure 12) resembles a usual curve if the input is an amplitude step B/A.

Since the studied method has a first-order transfer function, it can be controlled by a proportional regulator with or without integral.

By using the choice graph of the regulator proposed by the method of Broida, this process has no delay τ, and the ratio θ/τ will tend towards infinity. This corresponds to the domain of proportional actions. Thus, we can write

$$K(p) = \frac{\theta}{G_s \theta_d}. \tag{18}$$

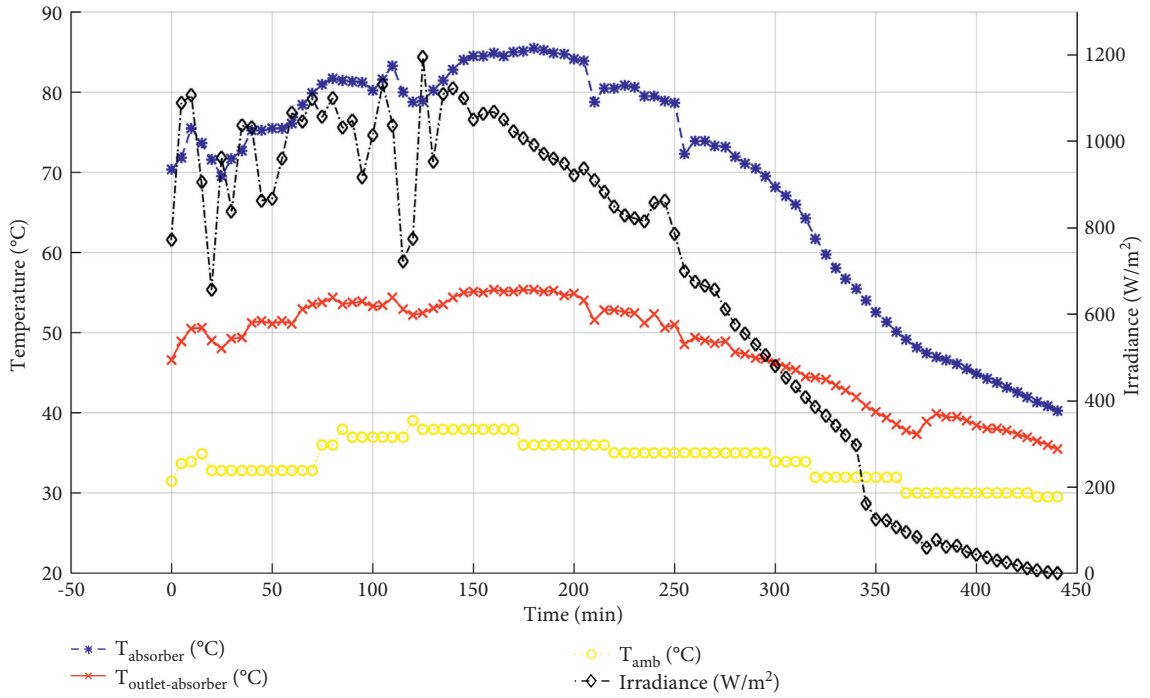

Figure 8: Temperature and irradiance profiles in dryer without regulation.

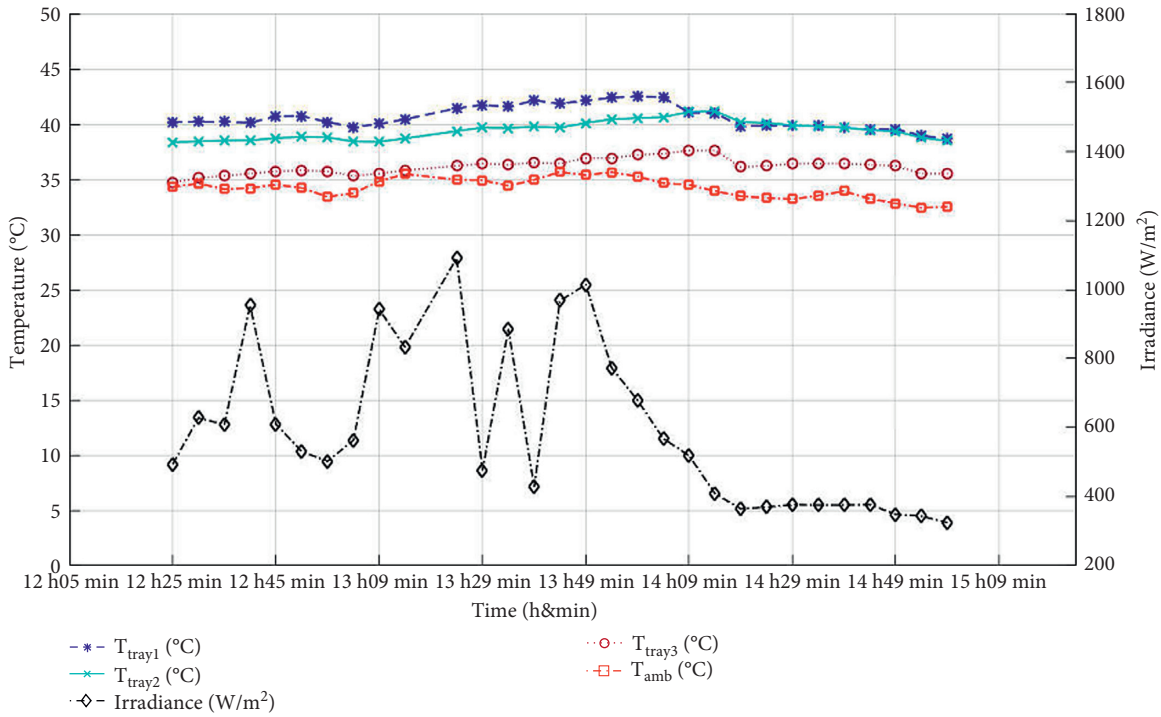

Figure 9: Temperature and irradiance profiles in crossing mode with regulation.

3.3. Control of Relative Humidity

3.3.1. Variation of Humidity during Temperature Control. Figure 13 shows that moisture curve varies in the opposite direction to the temperature. The humidity is stable at 10% after 4 hours, while the temperature also becomes stable at 56.4°C on the tray 2 after 2 hours. This shows that if the temperature is stable for a period of time, moisture will follow the same trend, and this information can be used to set the end of drying. This manipulation is done at the average relative humidity of 40%.

Table 2: Temperature reading on the trays in licking mode for different NTC positions.

Parameter	Mean and standard deviation			Set point	Mean ambient temperature	NTC position
	Tray 1	Tray 2	Tray 3			
Temperature (°C)	65.9 ± 2.3^{a}	61.5 ± 1.4^{b}	59.9 ± 1.4^{b}	60	42	Tray 3
	51.3 ± 1.5^{a}	52.18 ± 1.4^{a}	51.9 ± 1.2^{a}	52	41	Tray 2
	51.6 ± 1.5^{a}	53.4 ± 1.3^{b}	54.08 ± 1.37^{b}	51	41	Tray 1

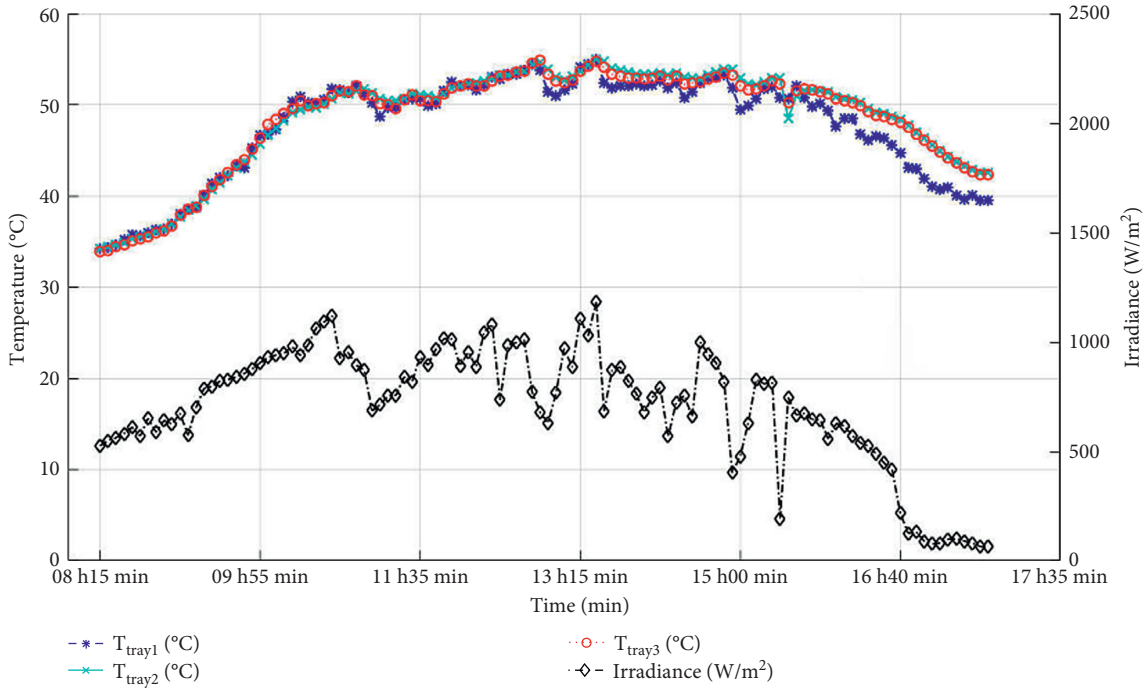

Figure 10: Temperature and irradiance profiles in linking mode.

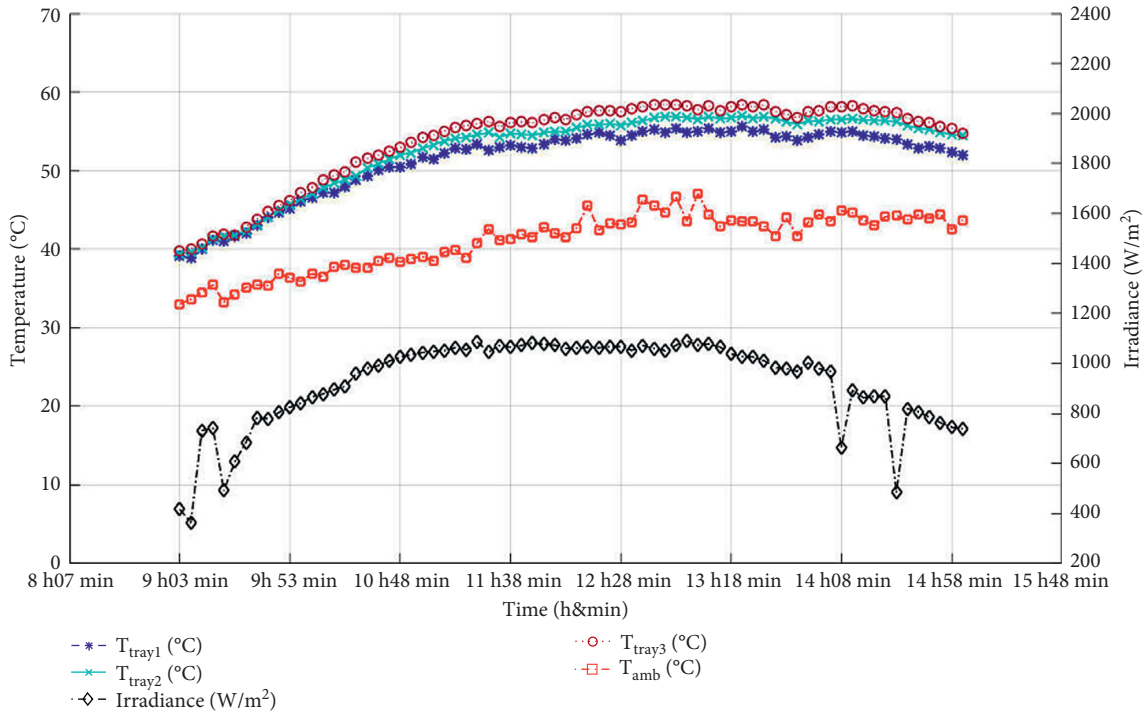

Figure 11: Temperature and irradiance profiles in mixed mode with regulation.

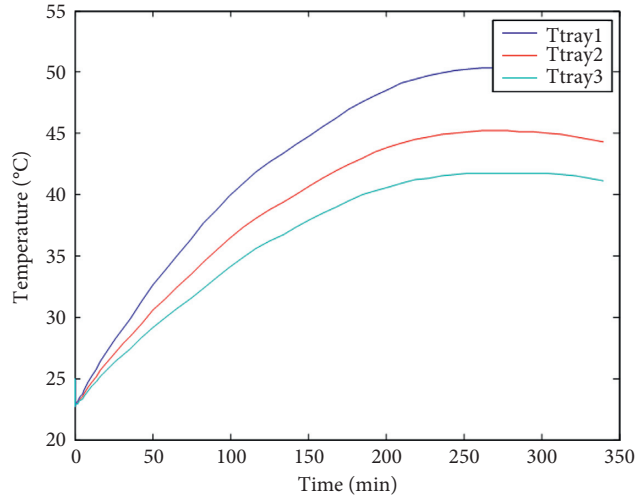

Figure 12: Experiment temperature profiles in the dryer chamber.

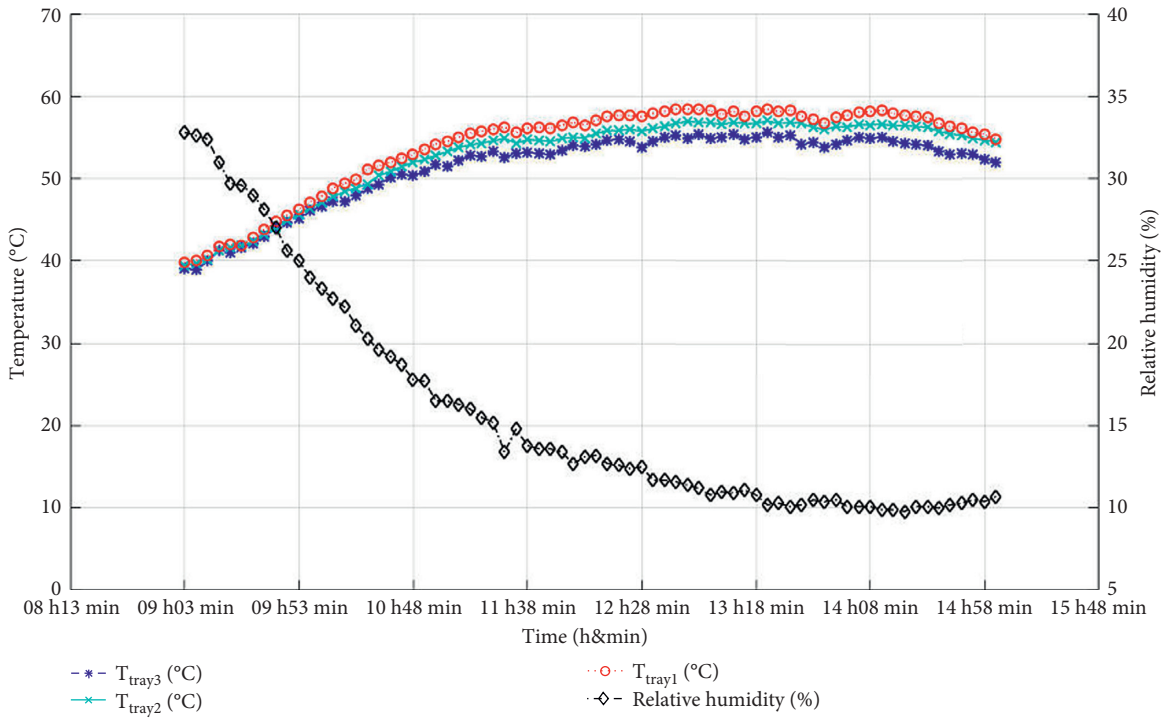

Figure 13: Temperature and irradiance profiles with regulation in the mixed mode.

3.3.2. Control the End of Drying. The majority of industrial drying systems makes it easy to control the parameters and sometimes offer the possibility to control several parameters simultaneously [27, 39]. These different parameters are controlled over time. Thus, time is considered as a control signal of drying. All food products use time to mark the end of their drying. The system may stop automatically if drying is complete.

In solar dryers where the energy source is not mastered, the heat source pumps the heat into the chamber to dry the products. Using the time to set the end of drying while the input parameters are stochastic can skew the results. The use of a system parameter to set the end of drying makes it possible to follow the stochastic variations of these parameters.

Relative humidity, which is a measurable, controllable, and stochastic quantity, can be used to control the drying of products. Indeed, it is possible to signal the end of drying of a product which has dried quickly or slowly.

4. Conclusion

For regulation to be possible in the indirect solar dryer, there must be solar energy that can exceed the set point temperature by more than 5%. With NTC fixed on tray number 2, the average temperature on three trays is 51.3 ± 1.5^{a}°C,

$52.18 \pm 1.4^{a°}$C, and $51.9 \pm 1.2^{a°}$C, respectively, and 51.86 ± 1.54°C, 51.60 ± 1.16°C, and 50.42 ± 1.13°C, respectively, when the set point is 52°C and 51°C in the linking and mixed air flow mode, respectively, whereas, in the crossing airflow mode, the temperature gradient does not allow regulation on all trays. During storage, the time constant C depends on the properties of the coolant and the convective exchanges, and it influences the rapid attainment of the maximum temperature.

In solar dryers where the energy source variation is stochastic, relative humidity, which is a measurable, controllable, and stochastic quantity is the best parameter to fix the end of drying products instead of time.

Data Availability

The data used to support the findings of this study are available from the corresponding author upon request.

Conflicts of Interest

The authors declare that they have no conflicts of interest.

References

[1] C. Bonazzi, E. Dumoulin, and J. J. Bimbenet, "The drying of food products," *Agricultural Food Industry*, vol. 125, no. 03–04, pp. 12–22, 2008.

[2] M. Sharma, "A review on developments in solar portable dryers," *Studies in Indian Place Names*, vol. 40, no. 48, pp. 1160–1182, 2020.

[3] M. C. Ndukwu, L. Bennamoun, and F. I. Abam, "Experience of solar drying in Africa: presentation of designs, operations, and models," *Food Engineering Reviews*, vol. 10, no. 4, pp. 211–244, 2018.

[4] P. Prouvost, "Instrumentation et régulation-2e éd," *En 30 fiches-Comprendre et s' entraîner facilement*, Dunod, Paris, France, 2015.

[5] G. B. Tchaya, E. Tchoffo Houdji, M. Garga, B. Kaldambe Zoua, and J. L. Nsouandélé, "Performance improvement of a hybrid biomass/indirect solar dryer (HBISD) for drying guava (psidium guajava)," *IJISET-International Journal of Innovative Science, Engineering & Technology*, vol. 8, no. 8, pp. 2348–7968, 2021.

[6] L. Bennamoun, M. Simo-Tagne, and M. C. Ndukwu, "Simulation of storage conditions of mixed biomass pellets for bioenergy generation: study of the thermodynamic properties," *Energies*, vol. 13, no. 10, p. 2544, 2020.

[7] S. N. Ndirangu, "Design and performance evaluation of an improved solar-biomass greenhouse dryer for drying of selected crops in western Kenya," *Agricultural Engineering International: CIGR Journal*, vol. 22, no. 3, pp. 219–229, 2020.

[8] G. B. Tchaya, M. Kamta, M. Havet, and C. Kapseu, "Thermal performance modelling of solar collector with heat storage," *International Journal of Engineering Systems Modelling and Simulation*, vol. 9, no. 1, pp. 53–62, 2017.

[9] G. B. Tchaya, J. H. Tchami, M. Kamta, and C. Kapseu, "Solar energy storage in an indirect solar dryer (ISD) with stone for drying in continuous," *Journal of Solar Energy Research*, vol. 3, no. 1, pp. 81–85, 2018.

[10] A. Oliver, F. J. Neila, and A. García-Santos, "PCM choosing and classification according to their characteristics for their application for thermal energy storage systems," *Materiales de Construcción*, vol. 62, no. 305, pp. 131–140, 2012.

[11] M. C. Ndukwu, L. Bennamoun, F. I. Abam, A. B. Eke, and D. Ukoha, "Energy and exergy analysis of a solar dryer integrated with sodium sulfate decahydrate and sodium chloride as thermal storage medium," *Renewable Energy*, vol. 113, pp. 1182–1192, 2017.

[12] M. C. Ndukwu, L. Bennamoun, and M. Simo-Tagne, "Reviewing the exergy analysis of solar thermal systems integrated with phase change materials," *Energies*, vol. 14, no. 3, p. 724, 2021.

[13] B. Kamkari and H. Shokouhmand, "Experimental investigation of phase change material melting in rectangular enclosures with horizontal partial fins," *International Journal of Heat and Mass Transfer*, vol. 78, pp. 839–851, 2014.

[14] A. Reyes, J. Vásquez, N. Pailahueque, and A. Mahn, "Effect of drying using solar energy and phase change material on kiwifruit properties," *Drying Technology*, vol. 37, no. 2, pp. 232–244, 2019.

[15] P. Cerezal Mezquita, A. Álvarez López, and W. Bugueño Muñoz, "Effect of drying on lettuce leaves using indirect solar dryer assisted with photovoltaic cells and thermal energy storage," *Processes*, vol. 8, no. 2, p. 168, 2020.

[16] L. Bennamoun and A. Belhamri, "Study of a solar batch dryer. Adaptation to local climate," in *Proceedings of the Heat exchange and renewable energy sources. International symposium*, pp. 221–228, Lille France, July 2002.

[17] J. Nganhou and T. Nganya, "Simulation numérique du comportement dynamique d'un système de séchage solaire de fèves de cacao au Cameroun," *Procédés biologiques et alimentaires*, vol. 1, 2002.

[18] L. Bennamoun, "Reviewing the experience of solar drying in Algeria with presentation of the different design aspects of solar dryers," *Renewable and Sustainable Energy Reviews*, vol. 15, no. 7, pp. 3371–3379, 2011.

[19] M. Simo-Tagne and M. C. Ndukwu, "Study on the effect of conical and parabolic solar concentrator designs on hybrid solar dryers for apricots under variable conditions: a numerical simulation approach," *International Journal of Green Energy*, vol. 18, pp. 1–19, 2021.

[20] M. Simo-Tagne, M. C. Ndukwu, and M. N. Azese, "Experimental modelling of a solar dryer for wood fuel in Epinal (France)," *Modelling-International Open Access Journal of Modelling in Engineering Science*, vol. 1, no. 1, pp. 39–52, 2020.

[21] M. C. Ndukwu, E. O. Diemuodeke, F. I. Abam, U. C. Abada, N. Eke-emezie, and M. Simo-Tagne, "Development and modelling of heat and mass transfer analysis of a low-cost solar dryer integrated with biomass heater: application for West African Region," *Scientific African*, vol. 10, Article ID e00615, 2020.

[22] M. Simo-Tagne, A. Tagne Tagne, M. C. Ndukwu et al., "Numerical study of the drying of cassava roots chips using an indirect solar dryer in natural convection," *AgriEngineering*, vol. 3, no. 1, pp. 138–157, 2021.

[23] A. Talla, Y. Jannot, C. Kapseu, and J. Nganhou, "Experimental study and modelling of the drying kinetics of tropical fruits: application to banana and mango. Food Science," *Science des Aliments*, vol. 21, no. 5, 2001.

[24] O. Yaldỳz and C. Ertekỳn, "Thin layer solar drying of some vegetables," *Drying Technology*, vol. 19, no. 3–4, 2001.

[25] M. Rivier, J.-M. Méot, T. Ferré, and M. Briard, *Drying of Mangoes*, Editions Quae, Versailles, France, 2009.

[26] L. M. Bal, S. Satya, and S. N. Naik, "Solar dryer with thermal energy storage systems for drying agricultural food products:

a review," *Renewable and Sustainable Energy Reviews*, vol. 14, no. 8, 2010.

[27] V. K. Sharma, A. Colangelo, and G. Spagna, "Experimental investigation of different solar dryers suitable for fruit and vegetable drying," *Renewable Energy*, vol. 6, no. 4, 1995.

[28] A. Sharma, C. R. Chen, and N. V. Lan, "Solar-energy drying systems: a review," *Renewable and Sustainable Energy Reviews*, vol. 13, no. 6–7, 2009.

[29] C. Bonazzi, E. Dumoulin, and J. J. Bimbenet, "The drying of food products," *Agricultural Food Industry*, vol. 125, 2008.

[30] A. Reyes, F. Cubillos, A. Mahn, and J. Vásquez, "Control system in a hybrid solar dryer," in *Proceedings of the 2014 5th International Renewable Energy Congress (IREC)*, pp. 1–5, Hammamet, Tunisia, March 2014.

[31] A. Abakarov, H. Jiménez-Ariza, E. Correa-Hernando et al., *Control of a Solar Dryer through Using a Fuzzy Logic and Low-Cost Model-Based Sensor*, in *Proceedings of the International Conference of Agricultural Engineering. CIGR-Ageng2012*, Valencia- España, July 2012.

[32] G. B. Tchaya, M. Kamta, and C. Kapseu, "Improvement of an indirect solar dryer with forced convection by variation of airflow mode," *International Journal of Emerging Technology and Advanced Engineering*, vol. 4, no. 1, pp. 518–522, 2014.

[33] M. Kamta, G. B. Tchaya, and C. Kapseu, "Performance of temperature controller for indirect solar dryers used on farms in tropical area," *Alternative Energy and Ecology (ISJAEE)*, vol. 91, no. 11, pp. 69–74, 2010.

[34] K. S. Ong, "Thermal performance of solar air heaters: mathematical model and solution procedure," *Solar Energy*, vol. 55, no. 2, pp. 93–109, 1995.

[35] P. Prouvost, "Automatique: contrôle et régulation: cours et exercices corrigés," Dunod, Paris, 2004.

[36] K. R. Arun, M. Srinivas, C. A. Saleel, and S. Jayaraj, "Active drying of unripened bananas (Musa Nendra) in a multi-tray mixed-mode solar cabinet dryer with backup energy storage," *Solar Energy*, vol. 188, pp. 1002–1012, 2019.

[37] A. E. Kabeel, P. D. L. Dharmadurai, S. Vasanthaseelan et al., "Experimental studies on natural convection open and closed solar drying using external reflector," *Environmental Science and Pollution Research*, pp. 1–10, 2021.

[38] M. Ayadi, I. Zouari, and A. Bellagi, "Simulation and performance of a solar drying unit with storage for aromatic and medicinal plants," *International Journal of Food Engineering*, vol. 11, no. 5, pp. 597–607, 2015.

[39] A. Zoukit, H. El Ferouali, I. Salhi, S. Doubabi, N. Abdenouri, and T. El Kilali, "Control of a solar dryer using a hybrid solar gas collector," in *Proceedings of the 2016 International Conference on Electrical Sciences and Technologies in Maghreb (CISTEM)*, pp. 1–6, Marrakech & Bengrir, Morocco, October 2016.